Spin torque oscillator for microwave assisted magnetic recording

Y. Sakuraba, S. Bosu, W. Zhou, H. Sepehri-Amin , S. Kasai and K. Hono
National Institute for Materials Sciece (NIMS), Sengen 1-2-1, Tsukuba, Ibaraki, Japan

Microwave assisted magnetic recording (MAMR) [1]is one of the potential techniques for the next generation high density magnetic recording up to 2T bit/in^2 and beyond [2]. MAMR is based on the principle where ac magnetic field ($\mu_0 H_{ac}$) generated from a spin torque oscillator (STO) is applied to the recording media having high thermal stability for lowering the switching field of magnetization of magnetic grains[3-5]. One major challenge for realizing MAMR is the development of a STO consisting of a field generating layer (FGL) having large magnetic volume and spin-injection layer (SIL) with device diameter size D ~ 30 to 40 nm that is able to generate a large enough $\mu_0 H_{ac}$ > 0.1 T from FGL with a frequency, f over 20 GHz at small bias current density J_C < 1.0 X 10^8 A/cm^2 [6, 7]. Particularly, the reduction of J_C is the most difficult task because the magnetic volume of FGL must be large for a sufficient ac magnetic field. Therefore, in our recent studies, we have fabricated various types of STO for MAMR having highly spin-polarized Heusler SIL layer to investigate the effect of spin-polarization on the oscillation dynamics in FGL layer. In order to simulate the behavior of STT-induced dynamics in the STO against various material parameters such as magnetization and spin-polarization, we employed a micromagnetic simulation using the code magnum.fe [8], which solves the coupled dynamics of magnetization (m) and the spin accumulation (s) simultaneously using the Landau Lifshitz Gilbert (LLG) equation and the time dependent 3D spin diffusion equation, respectively.

In this talk, we will show the result of two different STOs. First one has a perpendicularly magnetized Heusler SIL in which thin Heusler layer is deposited on perpendicular magnetized FePt. In this device, we clearly confirmed from both experiments and simulations that out-of-plane (OPP)-mode rf oscillation in FGL can be excited under lower J_C by using Heusler SIL compared with usual CoFe SIL.[9,10] The oscillation peak with the f of over 20 GHz was detected by slightly tilting magnetic field direction from the device normal (Fig.1). In order to reduce the total thickness of the STO device, we have recently fabricated the device with in-plane magnetized thin SIL, in which the synchronized OPP oscillation was predicted to generate between SIL and FGL by flowing electron from SIL to FGL.[11] The analysis of R-H curves under different current density with the micromagnetic simulations will be shown.

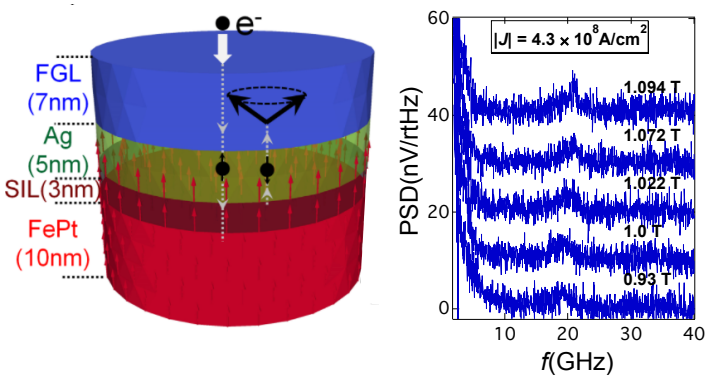

Figure 1. The stacking structure of STO for MAMR(Left), The rf spectra by applying magnetic field to 5 degree titled direction from the device normal (Right).[10]

[1] J.-G. Zhu, et al. IEEE Trans. Magn. 44, 125 (2008), [2] Y. Shiroishi, et al., IEEE Trans. Magn. 45, 3816 (2009)
[3] S. Okamoto, et al., Phys. Rev. Lett. 109, 237209 (2012), [4] C. T. Boone, et al., J. Appl. Phys. 111, 07B907 (2012)
[5] S. Okamoto, et al., J. Phys. D: Appl. Phys. 48, 353001 (2015), [6] A. Takeo, et al.,, Digest of Intermag Conference 2014 (AD-02), [7] M. Igarashi, Y. Suzuki, Y. Sato, IEEE Trans. Magn. 46, 3738 (2010)
[8]C. Abert, M. Ruggeri, F. Bruckner, C. Vogler, G. Hrkac, D. Praetorius, and D. Suess, Sci. Rep. 5, 14855 (2015)
[9] S. Bosu, et al., Appl. Phys. Lett. 108, 072403 (2016), [10] S. Bosu, et al., Appl. Phys. Lett. 110, 142403 (2017)
[11]J. Zhu, Joint MMM-Intermag Conf. 2016, AB11

スピントルク発振器を位相同期回路によって安定化した際の位相安定性の理論限界および物理的起源

田丸慎吾、久保田均、薬師寺啓、福島章雄、湯浅新治
（産総研　スピントロニクス研究センター）

Physical origin and theoretical limit of the phase stability of a spin-torque oscillator stabilized by a phase-locked loop

S. Tamaru, H. Kubota, K. Yakushiji, A. Fukushima, S. Yuasa
(AIST, Spintronics Research Center)

はじめに

スピントルク発振器(Spin torque oscillator, STO) は、微小な磁性体積層膜に直流電流を注入する事により磁化歳差運動を励起し、マイクロ波信号を発生するデバイスである。STO はそのサイズ(数 10~数 100 nm)、広い周波数可変帯域、半導体プロセスとの整合性等、従来の発振器には無い数々の利点を持つため、高周波集積回路内のマイクロ波信号源としての応用が期待されている。だが現時点では発振が不安定なため、まだ実用化には至っておらず、発振を安定化する技術が STO 実用化には必須となる。この問題を解決するため、我々は STO に特化した位相同期回路(Phase locked loop, PLL)を開発し、それを用いて STO を安定化したところ、マイクロ波領域において極めて鋭いスペクトルが観測され、STO の位相同期に成功したことが確認された[1]。しかしながら、そのピークの両側には市販の半導体 PLL 回路よりもまだずっと大きい残留位相ノイズも観測され、その為 STO を PLL で安定化しても、まだ実用化レベルまで性能が向上したとは言えない状況である。

実験及び解析方法

更なる性能改善の可能性を検証するため、PLL 回路の詳細な解析を行った。STO のフリーラン時の性能は、出力と位相安定性という 2 つの性能指標によって示される。出力が小さいと、それを増幅する増幅器の雑音が相対的に大きくなるため、信号雑音比が悪くなり、その結果ジッター増加や、カウントエラーが起きる。この出力とジッターやカウントエラーの関係を計算し、実験結果と比較したところ、図 1 に示す通り非常に良い一致が得られた[2]。次に STO フリーラン時の出力信号における周波数揺らぎのスペクトル密度(Frequency error spectral density, FESD)を計算し、この結果及び PLL の回路定数を用いて、STO が PLL によって安定化された際の残留位相エラーのスペクトルを計算し、実験結果と比較したところ、こちらも図 2 に示す通り非常に良い一致が得られた[3]。これらの結果は、STO のフリーラン時の性能指標から、PLL で位相安定化された際の性能を予測するための計算が定式化された事を示す。これらの解析結果により、FESD が STO の位相安定性の定量解析に必要である事、FESD は低周波では 1/f 揺らぎ、コーナー周波数以上では一定となり、それぞれ磁化構造の揺らぎ、STO フリー層の熱安定性が重要であることが示めされた。

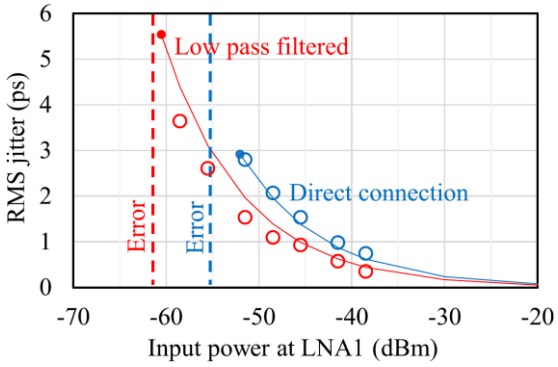

Fig. 1, ジッターやカウントエラーと STO 出力の関係の理論と実測値の比較

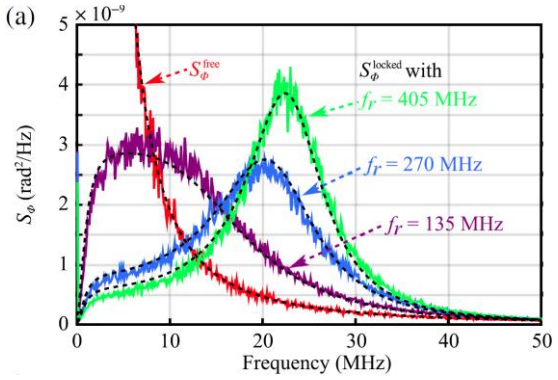

Fig. 2,フリーラン、位相同期時の STO 出力の FESD の理論と実測値の比較

参考文献

1) S. Tamaru et. al, Sci. Rep., 18134 (2015)
2) S. Tamaru et. al, Jpn J. Appl. Phys., 093003 (2016)
3) S. Tamaru et. al, Phys. Rev. Applied, accepted (2017)

Spin-orbit torque induced switching using antiferromagnets and its application to artificial neural networks

S. Fukami[1-4], A. Kurenkov[1], W. A. Borders[1], C. Zhang[1,2], S. DuttaGupta[1,3], and H. Ohno[1-5]
[1] Laboratory for Nanoelectronics and Spintronics, RIEC, Tohoku University, Sendai 980-8577 Japan
[2] Center for Spintronics Integrated Systems, Tohoku University, Sendai 980-8577 Japan
[3] Center for Spintronics Research Network, Tohoku University, Sendai, 980-8577 Japan
[4] Center for Innovative Integrated Electronic Systems, Tohoku University, Sendai 980-0845 Japan
[5] WPI-Advanced Institute for Materials Research, Tohoku University, Sendai 980-8577 Japan

Spin-orbit torque (SOT) induced switching, a magnetization switching technique utilizing spin-orbit interactions in heterostructures with broken space inversion symmetry, offers attractive avenues for high-performance and low-power integrated circuits [1-3]. While the heterostructure considered, in general, consists of a bilayer with a non-magnet (NM), e.g., Pt, Ta, and W, and a ferromagnet (FM), we here show that replacing the NM by an antiferromagnet (AFM) opens up various opportunities beyond the conventional integrated circuits [4-6].

SOT switching in AFM/FM heterostructures can be characterized by the following three effects. The first one is the spin Hall effect (SHE), which manifests in SOT. Several theoretical and experimental works revealed that noncollinear AFMs exhibit direct/inverse SHE. We find that, in a heterostructure consisting of an antiferromagnetic PtMn and a ferromagnetic Co/Ni multilayer, the PtMn exhibits SOT large enough to switch the magnetization of Co/Ni layer. The second effect is the exchange bias, which is known to arise at AFM/FM interfaces and manifests itself in an effective in-plane field. Whereas an application of in-plane field is necessary to achieve bipolar switching of perpendicular magnetization for NM/FM systems, the AFM/FM system allows field-free switching as a result of the exchange bias. The third effect, which arises in polycrystalline systems, relates to a variation of the exchange bias among the polycrystalline grains, which provide fine stable magnetic domain structures [5]. This leads to an analog-like switching behavior as is not usually observed in NM/FM structures. Thanks to these effects, the SOT switching in AFM/FM heterostructures not only offers promising route toward SOT-based magnetoresistive random access memory (SOT-MRAM), but also open unconventional paradigms such as neuromorphic computing.

Taking advantage of the analog nature of the SOT devices with the AFM/FM structure, we have shown a proof-of-concept demonstration of neuromorphic computing [6]. In this work, we have developed an artificial neural network using 36 AFM/FM-based SOT devices with a field-programmable gate array and software implemented on a PC, and have tested an associative memory operation. The Hopfield model [7] has been employed to associate memorized patterns from randomly generated noisy patterns. The learning operation based on the Hebbian rule is performed by changing the Hall resistance of analog SOT devices, which represents a synaptic weight between neurons. We have confirmed that the SOT devices have the expected learning ability, resulting in a successful associative memory operation [6]. Since the spintronics devices have virtually infinite endurance and nonvolatility, the spintronics-based artificial neural networks are expected to realize *edge* artificial intelligence with an on-chip learning capability.

This work is partly supported by ImPACT Program of CSTI, R&D Project for ICT Key Technology of MEXT, JST-OPERA, and JSPS KAKENHI Grant Number 17H06093.

Reference

1) I. M. Miron et al., Nature **476**, 189 (2011).
2) L. Liu et al., Science **336**, 555 (2012).
3) S. Fukami et al., Nature Nanotechnology **11**, 621 (2016).
4) S. Fukami et al., Nature Materials **15**, 535 (2016).
5) A. Kurenkov et al., Applied Physics Letters **110**, 092410 (2017).
6) W. A. Borders et al., Applied Physics Express **10**, 013007 (2017).
7) J. J. Hopfield, Proceedings of the National Academy of Sciences USA **79**, 2554 (1982).

Voltage-Control Spintronics Memory (VoCSM) for a High-density and High-speed Non-volatile Memory

Naoharu Shimomura, Hiroaki Yoda, Tomoaki Inokuchi, Katsuhiko Koi, Yushi Kato, Altansargai Buyandalai, Satoshi Shirotori, Yuuzo Kamiguchi, Kazutaka Ikegami, Soichi Oikawa, Hideyuki Sugiyama, Mariko Shimizu, Mizue Ishikawa, Tiwari Ajay, Yuichi Ohsawa, Yoshiaki Saito, and Atsushi Kurobe
Corporate Research & Development Center, Toshiba Corporation

1 Komukai, Toshiba-cho, Saiwai-ku, Kawasaki, Kanagawa Prefecture, 212-8582, Japan

Technology to reduce energy consumption of computing devices, and especially that of working memories such as DRAM and SRAM, is critically important because of the recent drastic increase in electric power usage due to the information explosion. MRAM is the sole candidate for a non-volatile working memory because it offers the possibility of fast switching and long life time. Application of MRAM to the working memories is a focus of high expectations because of the potential advantages in terms of low-power computing.

Spin Transfer Torque (STT) has been extensively investigated as an MRAM writing scheme. However, because a same current path is used both for reading and writing, scaling and endurance are limited by read disturbance and breakdown of the tunnel barrier of MTJs, respectively. Voltage-controlled-magnetic-anisotropy (VCMA) has been proposed as the ultimate power reduction scheme. It also improves the read disturbance and the endurance. However, it requires very precise control of write pulse duration time. Meanwhile, Spin Hall writing can prevent the read disturbance because different paths are used for writing and reading. However, there is a drawback in that shrinking the cell size is difficult because it requires at least two transistors for 1 bit memory cell.

We proposed Voltage-Control Spintronics Memory (VoCSM), an architecture combining VCMA and the Spin Hall effect [1)]. As illustrated in Fig. 1, multiple (for example, 8) MTJs are aligned on a heavy metal electrode that has strong spin-orbit interaction. VoCSM handles all 8 bits simultaneously by a single write pulse. In the 1st step, all 8 bits are set to one of the 2 bit data (for example, data “zero”) by applying the voltage on the MTJs and the current pulse on the electrode. The voltage is used to lower an energy barrier between two states of the MTJs by VCMA and the current pulse gives the spin torque on the MTJs by the Spin Hall effect to switch the magnetization. After that, in the 2nd step, the opposite data (“1” in this case) is written on the selected MTJs in the 8bit memory cells depending on the data set by applying the voltage to lower or raise the energy barrier of the MTJs and also the write current pulse in the opposite direction to that of the 1st step. This writing scheme reduces the power consumption because all 8 bits are written by the single write current pulse and moreover the write current itself is reduced by VCMA. VoCSM also enables shrinking of the cell size because one MTJ requires only one transistor.

We fabricated VoCSM TEGs to prove the concept. The MTJ structure was IrMn (8nm)/ CoFe (1.8nm)/ Ru (0.9nm)/ CoFeB (1.8nm)/ MgO (1.6nm)/ (CoFeB or FeB) (1.2~2.2nm)/ electrode and the MTJ size was about 50nm×150nm. We successfully demonstrated the magnetization switching of the selected MTJs on the electrode without switching unselected ones. We also demonstrated the fast switching with 5ns write pulses which is shown in Fig. 2. The measured write error rate with 5ns writing current pulses was lower than 1×10^{-6}.

This work was funded by the ImPACT Program of the Council for Science, Technology and Innovation (Cabinet Office, Government of Japan).

Reference

1) H. Yoda et al., Digests of IEDM, 27.6 (2016).

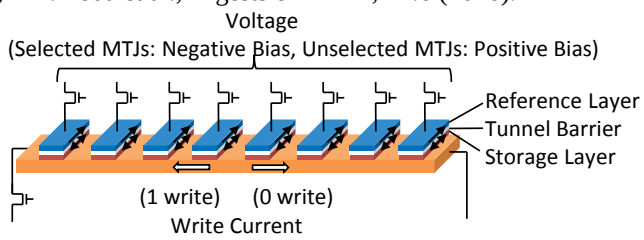

Fig. 1 Schematics of VoCSM

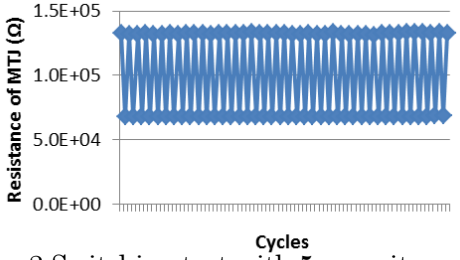

Fig. 2 Switching test with 5 ns write pulses

Magnetization switching by voltage controlled DMI

Hiroshi Imamura, Takayuki Nozaki, Shinji Yuasa, Yoshishige Suzuki
(Spintronics RC, AIST, Tsukuba, Ibaraki, Japan.)

Dzyaloshinskii-Moriya interaction is the anti-symmetric exchange interaction postulated by Igor Dzyaloshinskii in 1958[1]. Two years later Toru Moriya showed that the spin-orbit coupling is the microscopic mechanism of the antisymmetric exchange interaction [2]. The effects of the DMI on the magnetic properties of bulk materials have been extensively studied, e.g., the DMI is the source of the weak ferromagnetism of Fe2O3. Recently the voltage control of the DMI has attracted much attention as a tool for low power spin manipulation. One of the present authors showed that the Rashba spin-orbit interaction at the interface of the semiconductor nanostructures induces the interface DMI whose strength can be controlled by the gate voltage [3]. Very recently, Nawaoka et al. found that the DMI in the Au/Fe/MgO artificial multilayer can be controlled by application of a voltage [4].

The magnetic anisotropy (MA) is another magnetic property which can be controlled by the voltage. The voltage control of MA in a thin ferromagnetic film has attracted much attention as a key phenomenon for developing a voltage-controlled magnetic random access memory (MRAM) with low power consumption [5-9]. Shiota et al. demonstrated that the coherent magnetization switching is induced by application of voltage pulse to a few atomic layer of FeCo[4]. During the pulse application the magnetization coherently precesses around the effective magnetic field, and the magnetization switches if the pulse width is set to one-half period of the presession. However, since this is the toggle-mode switching, pre-reading is necessary for writing the MRAM. To avoid pre-reading it is necessary to develop a writing scheme based on the deterministic switching as shown in Fig. 1 (a), where the magnetization direction after the voltage pulse is determined by the polarity of the voltage and is independent of the initial magnetization direction.

Here we propose a new writing scheme of MRAM utilizing voltage-induced changes of MA and DMI. Based on the micromagnetics simulations we demonstrated that voltage-induced changes of MA and DMI can switch the magnetization of a perpendicularly magnetized right triangle deterministically; i.e., the magnetization direction is determined by the polarity of the voltage pulse

The system we consider is a perpendicularly magnetized right triangle (64 nm × 32 nm × 2 nm) shown in Fig. 1 (b). The micromagnetics simulations were performed by using the software package MuMax3[10]. The system is divided into cubic cells of side length 2 nm. The following material parameters are assumed: saturation magnetization Ms = 1.35 MA/m, exchange stiffness constant A = 10 pJ/m, Gilbert damping constant α = 1. The external field of 100 Oe was applied in the x-direction. The anisotropy constant (K) and the DMI constant (D) are assumed to vary with the applied

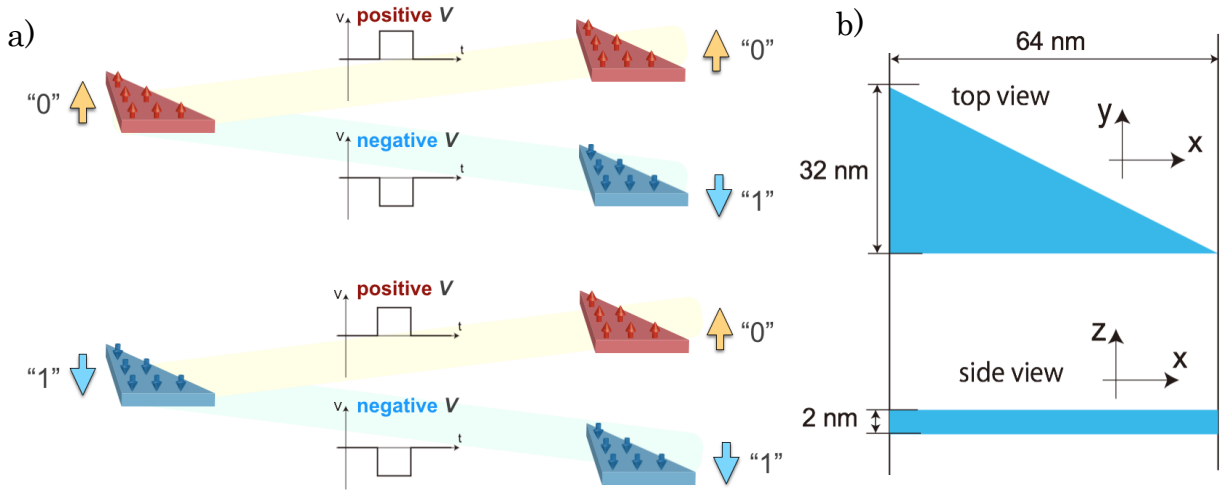

Fig. 1 a) Schematic illustration of the deterministic switching. The final magnetic state is determined by the polarity of the voltage pulse. b) Top and side views of the ferromagnetic triangle we simulated.

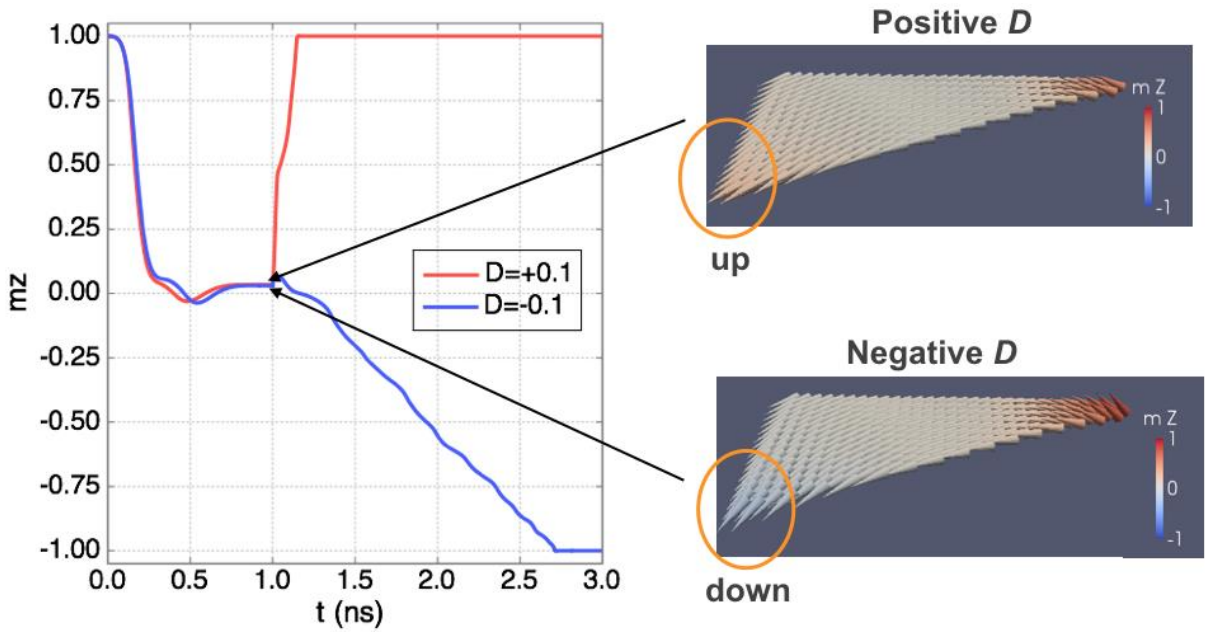

Fig. 2 Temporal variation of the z-component of the averaged magnetization, m_z, and snap shots of magnetization at the end of the pulse duration. The result for positive (negative) bias voltage is represented by the solid red (dotted blue) curves.

bias voltage in the different manner. In the absence of the applied voltage the anisotropy and DMI constants are K = 4 mJ/m2 and D = 0, respectively. When the positive (negative) bias voltage is applied they are K = 1.4 mJ/m2 and D = + (-) 0.1 mJ/m2. The width of the voltage pulse is 1 ns. The temperature is assumed to be zero.

The calculated results are shown in Fig. 2. The z-component of the averaged magnetization (m_z,) for the positive and negative bias voltage pulse are plotted by the solid (red) and dotted (blue) curves, respectively. The initial state is set as the perpendicularly polarized state with $m_z = 1$. Application of the voltage pulse for 1 ns tilts the magnetization to the in-plane direction and creates nucleation sites at the edges. The positive (negative) values of m_z are represented by red (blue) tones. The magnetization of the nucleation site at the left down edge points slightly down (up) for the positive (negative) bias voltage pulse due to the DMI as indicated by the circles on the snapshots. After 1 ns the bias voltage is turned off, and the magnetization relaxes to the perpendicularly magnetized state. The magnetization of the final state is the same as that of the nucleation site at the left down edge. Therefore the magnetization switches only if the negative bias voltage pulse is applied. For the initial state with $m_z = -1$ the magnetization switches only if the positive bias voltage pulse is applied. The systematic analysis for a wide range of parameters and conditions for switching will be presented.

Reference

1) I. Dzyaloshinskii, Journal of Physics and Chemistry of Solids 4, 241 (1958).
2) T. Moriya, Physical Review 120, 91 (1960).
3) H. Imamura, P. Bruno and Y. Utsumi, Phys. Rev. B 69, 121303 R (2004).
4) K. Nawaoka, S. Miwa, Y. Shiota1, N. Mizuochi and Y. Suzuki, Applied Physics Express 8, 063004 (2015) .
5) M. Weisheit, S. Fähler, A. Marty, Y. Souche, C. Poinsignon, and D. Givord, Science 315, 349 (2007).
6) D. Chiba, M. Sawicki, Y. Nishitani, Y. Nakatani, F. Matsukura, and H. Ohno, Nature 455, 515 (2008).
7) T. Maruyama, Y. Shiota, T. Nozaki, K. Ohta, N. Toda, M. Mizuguchi, A. A. Turapurkar, T. Shinjo, M. Shiraishi, S. Mizukami, Y. Ando, and Y. Suzuki, Nat. Nanotechnol. 4, 158 (2009).
8) Y. Shiota, T. Maruyama, T. Nozaki, T. Shinjo, M. Shiraishi, and Y. Suzuki, Appl. Phys. Express 2, 063001 (2009).
9) T. Nozaki, H. Arai, K. Yakushiji, S. Tamaru, H. Kubota, H. Imamura, A. Fukushima, and S. Yuasa, Applied Physics Express 7, 073002 (2014) .
10) A.Vansteenkiste, J. Leliaert, M. Dvornik, M. Helsen, F. Garcia-Sanchez and B. Van Waeyenberge, AIP Advances 4, 107133 (2014)

Voltage-induced precessional switching at zero bias magnetic field in a conically magnetized free layer

R. Matsumoto, T. Nozaki, S. Yuasa, and H. Imamura
(AIST)

Voltage-induced magnetization switching[1] at zero bias magnetic field has become one of the key requirements in developing voltage-torque magnetoresistive random access memory (MRAM). In the conventional magnetic tunnel junctions (MTJ) with the perpendicular magnetization, however, voltage-induced magnetization switching has been demonstrated under a bias magnetic field having in-plane (IP) component.[2,3] Instead of bias magnetic field, the IP component of the shape anisotropy field, H_k, has been often used. Finite H_k is commonly obtained in a ferromagnet having an elliptic-cylinder shape. In the case of a perpendicularly magnetized free layer, however, the shape anisotropy field cannot move the magnetization from the equilibrium state because H_k is zero at $(m_x, m_y, m_z) = (0, 0, \pm 1)$ where m_x and m_y (m_z) are IP (perpendicular) components of the unit magnetization vector ($\boldsymbol{m}$) of the free layer (see Fig. 1(a)). Tilting the angle of the magnetization from the perpendicular direction is also necessary for switching of the free layer magnetization.

To tilt the magnetization, we propose the usage of a cone state. Cone state is the magnetization state (see Fig. 1(b)) where the tilted magnetization is stabilized by the competition between the first- and the second-order magnetic anisotropy energies, $K_{1,\mathrm{eff}}$ and K_{u2}.[4,5] Here $K_{1,\mathrm{eff}}$ is the effective anisotropy constant, where demagnetization energy is subtracted from the first-order anisotropy constant (K_{u1}). The MTJ we assume is illustrated in Fig. 1(a). x-axis is parallel to the major axis of the ellipse. In our case,[6] $(m_x, m_y, m_z) = (0.322, 0, 0.947)$ in the equilibrium state. The voltage-induced dynamics is analyzed with the following Landau-Lifshitz-Gilbert (LLG) equation, $d\boldsymbol{m}/dt = -\gamma_0 \boldsymbol{m} \times [\boldsymbol{H}_{\mathrm{eff}} + \alpha(\boldsymbol{m} \times \boldsymbol{H}_{\mathrm{eff}})]$, where t is time, γ_0 is the gyromagnetic ratio, α is the Gilbert damping constant, and $\boldsymbol{H}_{\mathrm{eff}}$ is the effective magnetic field defined as $\boldsymbol{H}_{\mathrm{eff}} = -(1/(\mu_0 M))\nabla E$. Here, E is the energy density of the free layer at a finite voltage given by $E = (1/2)\mu_0 M_s^2(N_x m_x^2 + N_y m_y^2 + N_z m_z^2) + K_{u1}(1 - m_z^2) + K_{u2}(1 - m_z^2)^2$, where μ_0 is the vacuum permeability, M_s is the saturation magnetization, and N_x, N_y and N_z are demagnetization coefficients. In Fig. 1(c), an example of the simulation results is shown. The oscillation of m_z extends from positive to negative region. It indicates that voltage-induced precessional switching at zero bias magnetic field is available in a conically magnetized free layer with the elliptic-cylinder shape.

This work was partly supported by the ImPACT Program of the Council for Science, Technology and Innovation

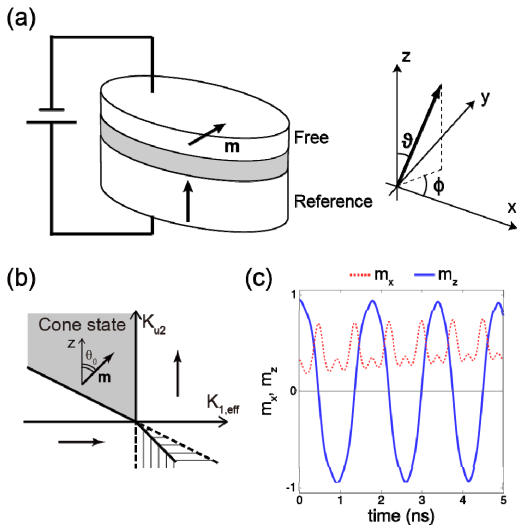

Fig. 1 (a) MTJ we assume. (b) Phase diagram of magnetic film with uniaxial anisotropy constants $K_{1,\mathrm{eff}}$ and K_{u2}. (c) Time evolution of m_x and m_z under application of voltage.

Reference

1) Y. Shiota et al: *Nat. Mater.*, 11, 39 (2012).
2) S. Kanai et al: *Appl. Phys. Lett.*, 101, 122403 (2012).
3) Y. Shiota et al: *Appl. Phys. Express*, 9, 013001 (2015).
4) D. Apalkov and W. Butler, US Patent 8,780,665 (2014).
5) R. Matsumoto et al: *Appl. Phys. Express*, 8, 063007 (2015).
6) The example of the parameters of the conically magnetized free layer in this study: $M_s = 1400$ kA/m, $\alpha = 0.005$, $K_{u1} = 1081$ kJ/m^3, and $K_{u2} = 193$ kJ/m^3 at zero voltage. $K_{u1} = 1051$ kJ/m^3, and $K_{u2} = 43$ kJ/m^3 under the application of a voltage. The volume of the free layer is $32 \times 16 \times \pi \times 1$ nm^3.

鋼板スリット部からの欠陥信号のモデル化

田中諒、笹山瑛由、圓福敬二
（九州大学）

Modeling of defect signal from slit part of steel plate

R. Tanaka, T. Sasayama, K. Enpuku
(Kyushu University)

はじめに

鋼材は高い透磁率を持つため、表皮深さが非磁性の金属に比べて浅くなる。よって渦電流探傷法を用いた鋼材の内部のきずの検出には低周波を用いる必要がある。これまで、三次元有限要素法による電磁界シミュレーションによって、鋼材裏面のスリット状の亀裂を低周波渦電流探傷法によって検出できる可能性を示した。本研究では、さらに、同様の手法で亀裂の高さによる信号の変化を求めた。また、得られた結果を Cole-Davidson の式でフィッティングを行った。

シミュレーション方法

Fig.1 に示すような 2 つの励磁コイルを鉄板の上側に平行に配置した場合の電磁界シミュレーションを行った。コイルと鉄板の距離 Z（リフトオフ）は 5 mm であり、2 つのコイル中心間の距離は 95 mm とした。コイルの寸法は内径が 35 mm、外径が 45 mm、高さが 3 mm とし、巻数は 18 turn とした。励磁電流の振幅は 1 A、周波数 f は 0~40 Hz として解析をした。なお、電流の方向は 2 つのコイルでは逆向きとした。

検査対象物は板厚が 10 mm の鋼板(SM490A)を用いた。鋼板の裏面に、励磁方向と平行、および垂直方向に縦 20 mm、横 5 mm のスリット状の亀裂を設けた。亀裂の高さ d はそれぞれ 2、4、6、8、10 mm である。各 d について、xy 平面上(Z = 5 mm)における亀裂によってのみ発生する z 軸方向の磁束密度分布を求め、その空間分布における最大値$\Delta B_z(f)$を求めた。

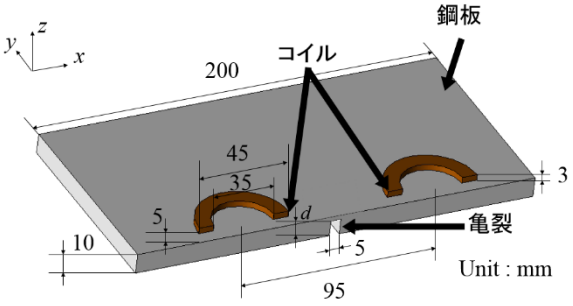

Fig.1　解析モデル（1/2 モデル）

シミュレーション結果

Fig.2 に周波数 f を 0 から 16 Hz まで変化させた場合の$\Delta B_z(f)$をそれぞれの亀裂高さ d について求めたグラフを示す。横軸に$\Delta B_z(f)$の実部、縦軸に$\Delta B_z(f)$の虚部を示す。グラフに示している数字は周波数を示す。亀裂高さによって周波数特性が違う事が分かる。

また Fig.3 にそれぞれの亀裂の高さにおいて$\Delta B_z(f)$を$\Delta B_z(0)$で規格化したもの（○印）を、Cole-Davidson の式でフィッティングした結果（×印）を示す。Fig.3 から分かるように、どの亀裂高さにおいても、14 Hz 以下ではおおよそフィッティングに成功した。

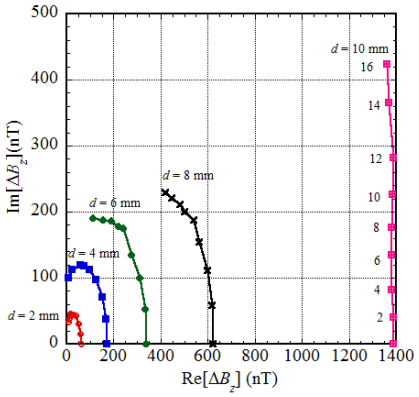

Fig.2　亀裂高さによるΔB_z

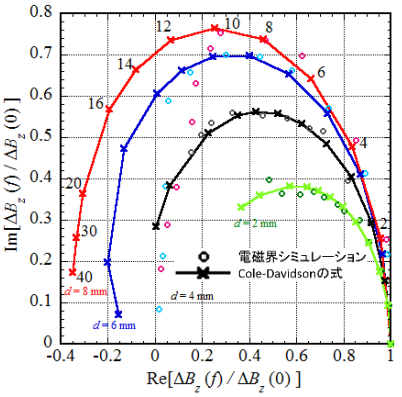

Fig.3　Cole-Davidson の式によるフィッティング

バックライト一体型 MO イメージングプレートを用いた 円偏光変調法による大面積の磁場分布の定量測定法の開発

長久保洋介、佐々木教真*、目黒栄**、西川雅美、石橋隆幸
（長岡技科大、*（株）オフダイアゴナル、**ネオアーク（株））

Development of quantitative measurement method for large area magnetic field distribution using MO imaging plate with backlight utilizing polarization modulation method

Y. Nagakubo, M. Sasaki*, S. Meguro**, M. Nishikawa, T. Ishibashi
(Nagaoka Univ. of Tech., *OFFDIAGONAL Co., Ltd., **Neoark Corp.)

我々は、大面積（数十 cm～1 m）の磁場分布を短時間で測定可能な磁気光学(MO)イメージング技術の開発を行っている。これまでに、磁気光学特性の優れた大面積ガーネット膜の開発 [1]およびϕ3 inch サイズの反射型イメージング装置の開発に成功している。さらに、イメージング領域の大面積化を可能とする、バックライト一体型 MO イメージングプレートを開発することにも成功した [2]。しかし、これらの方法では磁場の値を光強度と磁場強度の関係から求めるため、光学系の位置や光源の強度が変わるとその都度校正値を取り直す必要があった。そこで本研究では、校正値を用いずに磁気光学効果を定量的に計測可能な円偏光変調法 [3]とバックライト一体型 MO イメージングプレートを組み合わせた MO イメージング技術を開発した。

Fig. 1 に開発した MO イメージング装置の概略図を示す。MO イメージングプレートは、EL シート(EL-A6-SET、ルミテクノ)の上に偏光板とガーネット膜を重ねた構造とし、計測部として、カメラにλ/4 板と検光子を組み合わせた。MO イメージングプレートの裏側に置かれた測定対象物が作る磁場分布は、ガーネット膜に磁気的に転写される。そして、λ/4 板の光学軸を　-45º、0º、45º の角度として 3 枚の画像を計測した後、すべての画素における光強度から、次式によりファラデー回転角が得られる。

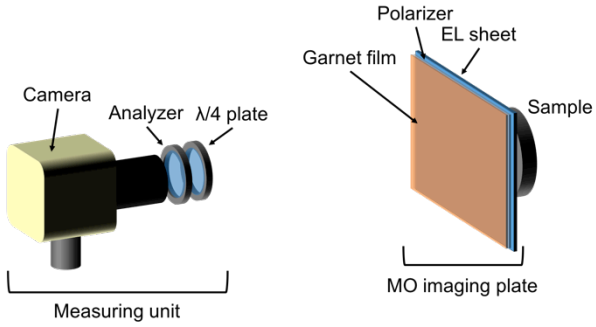

Fig. 1 Schematic illustration of the experimental setup.

$$\theta_F = \frac{2I_0\text{-}(I_{45} + I_{\text{-}45})}{2(I_{45} + I_{\text{-}45})} \qquad (1)$$

ここで、$I_{\text{-}45}$, I_0, I_{45} は、λ/4 板の角度が-45º、0º、45º の時に測定された画像の光強度である。磁場の値はガーネット膜のファラデー回転角と磁場の関係から求められる。

Fig.1 に、フェライト磁石について測定した磁場分布像を示す。フェライト磁石の磁場分布が明瞭に観察されているのがわかる。得られた磁場の値は、ガウスメーターで測定した値と一致したことから、校正値を用いずに定量的な磁場分布計測が可能であることが確認できた。

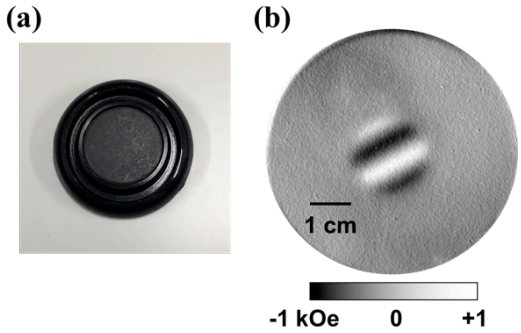

Fig. 2 (a) Digital photograph and (b) MO image of a ferrite magnet.

本研究の一部は、名大未来材料・システム研究所との共同研究及び文科省「ナノテクノロジープラットフォーム」の支援を受けて行われた。

参考文献

1)　T. Ishibashi, et al., Sensors and Materials, **27**, 965 (2015).
2)　長久保洋介 他, 第 64 回応用物理学会春季学術講演会, 16a-423-9.
3)　T. Ishibashi, et al., J. Appl. Phys. **100**, 093903 (2006).

J-PARC MLF における偏極パルス中性子イメージング技術の開発

廣井孝介、篠原武尚、林田洋寿*、Joseph Don Parker*、蘇玉華、及川健一、甲斐哲也、鬼柳善明**
（日本原子力研究開発機構 J-PARC センター、*総合科学研究機構、**名古屋大学）

Development of Polarized Pulsed Neutron Imaging Technique at MLF J-PARC

K. Hiroi, T. Shinohara, H. Hayashida*, J. D. Parker*, Y. Su, K. Oikawa, T. Kai and Y. Kiyanagi**
(J-PARC Center JAEA, *CROSS, **Nagoya University)

はじめに

現在、我々は J-PARC センター 物質・生命科学実験施設（MLF）において、偏極パルス中性子を用いた磁気イメージング手法の開発を行っている。本手法は、中性子ビーム経路内の磁場による中性子スピンのラーモア歳差回転に伴う中性子偏極度の変化を中性子２次元検出器を用いて取得し、そのエネルギー（波長）依存性を位置毎に解析することで中性子が感じた磁気情報を定量的に評価するものである。本手法の特徴は、プローブとなる中性子ビームの高い物質透過能力により、比較的大きな固体試料内部の磁気情報を取得できる点や、物質中と空間中両方の磁束密度をベクトル情報として定量的に評価できる点、さらに、他の磁気イメージング手法に比べ、一度に観察できる視野範囲が数 cm 四方と広い点が挙げられる。これらの特徴から、本手法は他の磁気イメージング手法では困難であった稼働状態での磁場関連機器内部の磁場観察への応用が期待されている。そのため、我々は時間変動する交流磁場を解析する手法や観察視野の拡大など、本手法を磁場関連製品の観察技術として実用化するため技術開発を進めてきた。本発表では、MLF において開発が進められている偏極パルス中性子を利用した磁気イメージング手法の概要と、それを利用した幾つかの応用研究の結果を説明する。

実験方法

偏極パルス中性子イメージングは MLF の BL22 に設置された、エネルギー分析型中性子イメージング装置「螺鈿」にて実施した。螺鈿におけるイメージング用偏極度解析装置の模式図を Fig. 1 に示す。この装置では、偏極子および検極子に V 型磁気スーパーミラーキャビティを使用した。中性子波長約 1.5～8 Å の範囲での偏極度解析が可能であり、画角約 40 mm 四方の偏極度分布像を取得できる。試料スペースの前後には中性子スピンの向きを回転させる２組のスピン回転子が設置されており、任意の方向に中性子スピンを制御することで、3 次元での偏極度解析が可能である。これにより、試料空間内の磁束密度の３次元ベクトル情報を取得する。現在、我々はこのイメージング用偏極度解析装置を利用して、稼働状態の小型モーターの磁場の観察や、トランス模擬試料からの漏洩磁場の観察、方向性電磁鋼板の磁区観察等の応用研究を実施しており、その結果を紹介する。

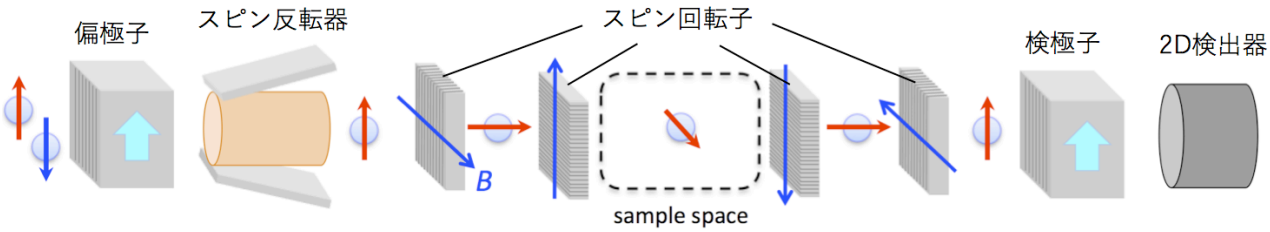

Fig.1　中性子イメージング用偏極度解析装置の模式図

謝辞

本研究は文部科学省 光・量子融合連携研究開発プログラム「実用製品中の熱、構造、磁気、元素の直接観察による革新エネルギー機器の実現」により実施された。